

Dynamics of Monochromatically Generated Nonequilibrium Phonons in $\text{LaF}_3:\text{Pr}^{3+}$

W. A. Tolbert,^(a) W. M. Dennis, and W. M. Yen^(a)

Department of Physics and Astronomy, University of Georgia, Athens, Georgia 30602

(Received 9 April 1990)

The temporal evolution of nonequilibrium phonon populations in $\text{LaF}_3:\text{Pr}^{3+}$ is investigated at low temperatures (1.8 K) utilizing pulsed, tunable, monochromatic generation and time-resolved, tunable, narrow-band detection. High-occupation-number, narrow-band phonon populations are generated via far-infrared pumping of defect-induced one-phonon absorption. Time-resolved, frequency-selective detection is provided by optical sideband absorption. Nonequilibrium phonon decay times are measured and attributed to anharmonic decay.

PACS numbers: 63.20.Hp, 63.20.Mt, 78.50.Ec

The mechanism utilized for the monochromatic, volume generation of nonequilibrium phonons in previous investigations of acoustic-phonon dynamics is one-phonon emission from a resonant electronic level.¹ Non-radiative relaxation via this mechanism occurs within an optically pumped excited-state manifold² when the level separation is less than the Debye energy. Far-infrared (FIR) pumping of a ground-state level³ enhances the energy efficiency of optical generation by a factor of 10^3 , the energy ratio of an optical to FIR photon. The resonant nature of these generation mechanisms precludes tunable generation, without such external perturbations as mechanical stress or magnetic fields.

In this work, tunable, monochromatic volume generation of phonons is clearly demonstrated and is attributed to defect-induced one-phonon absorption, the mechanism responsible for the one-phonon absorption band observed in type-1 diamond.⁴ In a recently reported work in CaF_2 ,⁵ a fixed-frequency, continuous-wave, FIR laser-induced signal, on a large nonresonant background, was attributed to this mechanism. The presence of a heavy-mass defect (impurity ion) relaxes wave-vector conservation, enabling photons to couple directly to acoustic phonons of the same energy,⁶ a mechanism forbidden in a perfect lattice. This permits monochromatic phonon generation throughout the acoustic band with a tunable FIR source [Fig. 1(a)]. We present here an investigation of the phonon dynamics of $\text{LaF}_3:\text{Pr}^{3+}$ (0.5%), which we believe to be the first investigation of acoustic-phonon dynamics utilizing this generation mechanism.

It should be noted that the vibrational modes of a doped crystal are perturbed from those of the perfect lattice.⁶ For $\text{LaF}_3:\text{Pr}^{3+}$, however, the mass defect is $< 2\%$ and bond strengths are nearly equivalent due to the chemical similarity of Pr^{3+} and La^{3+} . Therefore, the perturbations to the phonon density of states⁷ and to the amplitudes and frequencies of the modes⁶ in the vicinity of impurity ions are very small. Also, resonant modes do not occur in systems with such a small mass defect.⁷

Our FIR source for phonon generation is a transversely excited atmospheric-pressure CO_2 laser-pumped molecular superradiant cell yielding line-tunable (8–238

cm^{-1}),⁸ narrow-bandwidth (< 500 MHz), temporally short (< 40 ns), high-power (1–10 mJ) pulses. An off-axis parabolic mirror is used to focus the FIR beam to a 2-mm spot size at the sample, which was immersed in a 1.8-K liquid-helium bath. The FIR pulse energies at the sample were in the range 0.1–1 mJ.

Phonon detection via optical pumping of the anti-Stokes absorption sideband of an impurity level, as suggested by Orbach,⁹ has been demonstrated to be extremely sensitive.¹⁰ Anti-Stokes implies the annihilation of phonon while Stokes implies phonon creation. In this work, phonons are detected by optically probing the anti-Stokes sideband of the 3H_4 - 3P_0 transition in Pr^{3+} [Fig. 1(b)]. Absorption of the optical probe pulse can occur only in the presence of phonons with energy Δ , the detuning of the probe from the zero-phonon line. The 3P_0 - 3H_6 fluorescence provides a monitor of the 3P_0 population and hence the phonon occupation number. The optical probe for phonon detection is a Nd-doped

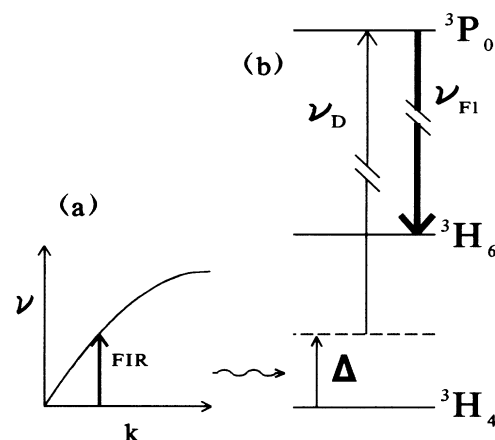


FIG. 1. (a) Schematic of phonon dispersion curve. FIR phonon generation via defect-induced one-phonon absorption is symbolized by the vertical arrow. (b) Energy level diagram for Pr^{3+} in LaF_3 . Phonons of energy Δ are detected via anti-Stokes absorption at the optical probe frequency ν_D , where $\Delta + \nu_D$ is the energy of the zero-phonon line. Phonon-induced absorption is monitored by observing the ν_{FI} fluorescence.

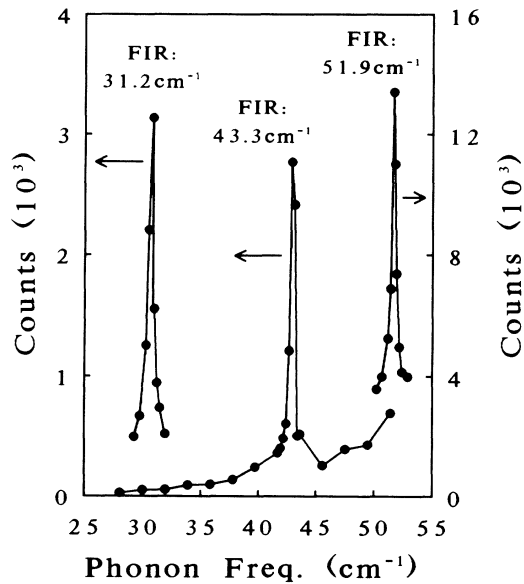


FIG. 2. Monochromatic phonon generation is demonstrated by plotting phonon-induced fluorescence as a function of phonon frequency, at fixed 40-ns optical gate delay. Note that the 31.2- and 51.9- cm^{-1} data have been vertically offset by 400 and 2400 counts, respectively. The solid lines connecting the data points are added as a guide to the eye.

yttrium-aluminum-garnet-pumped dye laser which generates 5-ns, 500- μJ pulses with 0.3- cm^{-1} bandwidth. The optical pulses are focused to a 100- μm spot size at the sample in a direction counterpropagating to the FIR pulses. The time-integrated, phonon-induced fluorescence is collected at 90°, spectrally filtered, and detected by photon counting the signal from a photomultiplier tube.

The temporal evolution of the nonequilibrium phonon populations can be observed by utilizing this absorption sideband technique in an "optical boxcar" scheme. In analogy with an electronic boxcar, the optical probe pulse acts as an "optical gate" for phonons of energy Δ . As the delay of this gate is scanned in time after the phonon-generating pulse, the fluorescence signal maps out the transient phonon population. Alternately, the spectral distribution of phonons can be obtained by scanning the detection frequency Δ (detuning), while the delay of the optical gate is held fixed.

Monochromatic phonon generation at three FIR frequencies is demonstrated in Fig. 2. At a fixed delay of 40 ns, the detection frequency Δ is scanned through each of the generation frequencies. Note that phonon population peaks at the FIR frequency and that the observed width is just that of our spectral resolution.

The generation of monochromatic phonon populations at several frequencies throughout the acoustic spectrum provides us with a unique opportunity to investigate the phonon dynamics in this system. Typical phonon transient data are shown in Fig. 3. The detection frequency

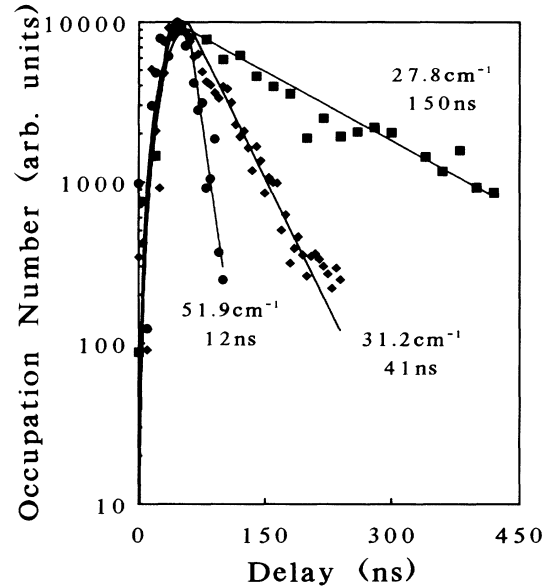


FIG. 3. Phonon occupation number plotted as a function of delay for three phonon frequencies. Detection frequency Δ is equal to generation frequency for each data set, and the 31.2- and 27.8- cm^{-1} phonon transients have been normalized to that of 51.9 cm^{-1} . The solid lines represent the best fits, as described in the text.

Δ is equal to the generation frequency in each trace and the peak signals have been normalized to the 51.9- cm^{-1} data for comparison. The solid lines are the analytic solutions to the phonon-occupation-number rate equation

$$dn(\Delta)/dt = -R_{\text{anh}}n(\Delta) + P(t)$$

that best fit the data. $n(\Delta)$ is the occupation number of phonons with energy Δ ; $R_{\text{anh}} = 1/\tau_{\text{anh}}$, the only fit parameter, is the anharmonic decay rate of these phonons; and $P(t)$ is the FIR pumping term. The presence of a fluorescence signal that persists for times longer than the FIR pulse width, and the absence of signal observed with FIR pumping above the acoustic band demonstrate that two-photon absorption (optical plus FIR) is not a significant process in this experiment.

Phonon decay times provided by these fits (circles) are plotted as a function of phonon frequency in Fig. 4. Previously reported anharmonic decay times for phonons in this system^{10,11} are denoted by squares. These data are in good agreement with the theoretical Δ^{-5} dependence of the anharmonic decay time predicted by the isotropic dispersionless model,¹² represented by the solid line. This frequency dependence has also been observed in CaF_2 .¹³ Nonradiative relaxation of an optically pumped electronic level is the phonon generation mechanism utilized by Refs. 10 and 11 and is, as described above, a well-established phonon source for the investigation of nonequilibrium phonon dynamics. The good agreement with these results indicates that defect-induced one-phonon absorption is a similarly appropriate phonon

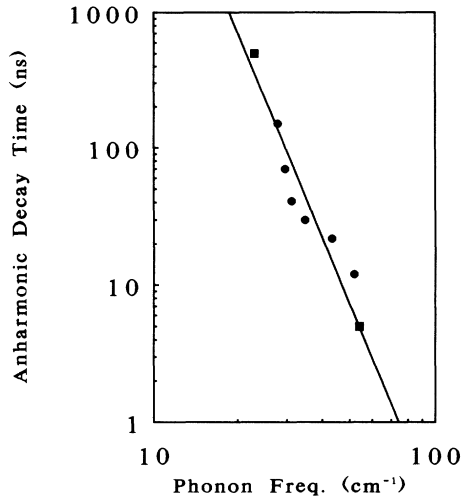


FIG. 4. Anharmonic decay time plotted as a function of phonon frequency demonstrating good agreement with the theoretical Δ^{-5} dependence of anharmonic decay time, represented by the solid line. Data from this work are represented by circles and the squares denote data from Refs. 10 and 11.

source.

Phonon occupation numbers can be obtained, at low temperatures, from the ratio of the phonon-induced anti-Stokes signal to that observed by optically pumping the Stokes absorption sideband of the zero-phonon line, in the absence of nonequilibrium phonons.¹⁰ Further, we expect the phonon generation width to be that of the FIR laser, while the detection width is given by the optical probe. Therefore, scaling by the ratio of these widths, we estimate occupation numbers $\bar{p}(\Delta)$ to be of order 10.

The rate equation used above to fit the phonon transient data can be simplified, under the assumption of steady-state pumping, to an expression for the absorption coefficient $\alpha(\Delta)$ in terms of occupation number $\bar{p}(\Delta)$. This is a good approximation in the case of 51.9-cm^{-1} phonon generation. We estimate $\alpha(51.9) = 2.4\text{ cm}^{-1}$ from $\alpha(\Delta) = h\Delta\bar{p}\Sigma/I_{\text{FIR}}T_{\text{ph}}$, where h is Planck's constant, $\Sigma = 1.7 \times 10^{18}\text{ modes/cm}^3$ is the number of resonant modes per unit volume,¹⁴ $I_{\text{FIR}} = 6 \times 10^5\text{ W/cm}^2$ is the FIR intensity, and $T_{\text{ph}} = 12\text{ ns}$ is the observed phonon decay time from Fig. 3. This is in good agreement with Ref. 15.

We have observed monochromatic phonon generation at several frequencies (27.8, 29.5, 31.2, 33, 34.5, 34.7, 43.3, 51.9, and 66 cm^{-1}). This range represents a significant fraction of the zone. The efficiency of both generation and detection increases with frequency as Δ^2 , making this combination of techniques particularly well suited to the investigation of phonons in the dispersive

regime.

In conclusion, FIR-pumped defect-induced one-phonon absorption has been demonstrated to be a convenient phonon source in the investigation of nonequilibrium phonon dynamics in this system and should be applicable to a wide variety of materials. We are currently utilizing this technique to investigate the spectral dynamics associated with the anharmonic decay of monochromatic phonon populations.

We thank R. S. Meltzer for many useful discussions and U. Happek for sending a preprint of recent work. We also wish to thank W. E. Bron for comments. This work is supported in part by the National Science Foundation, Grant No. DMR 8717696. One of us (W.M.D.) would like to thank the University of Georgia Research Foundation and the Office of the Vice President for Research, University of Georgia, for equipment funds.

(a)Also at Department of Physics, University of Wisconsin, Madison, WI 53705.

¹See, for example, K. F. Renk, in *Nonequilibrium Phonon Dynamics—1984*, edited by W. E. Bron, NATO Advanced Study Institutes, Ser. B, Vol. 124 (Plenum, New York, 1985), p. 59.

²W. M. Yen, W. C. Scott, and A. L. Schawlow, *Phys. Rev.* **136**, A271 (1964).

³W. A. Tolbert, W. M. Dennis, R. S. Meltzer, and W. M. Yen, *J. Lumin.* **45**, 153 (1990).

⁴R. Robertson, J. J. Fox, and A. E. Martin, *Philos. Trans. Roy. Soc. Ser. A* **232**, 463 (1934).

⁵U. Happek, T. P. Lang, and K. F. Renk, in *Phonons '89*, edited by S. Hunklinger, W. Ludwig, and G. Weiss (World Scientific, Singapore, 1990), p. 1427.

⁶P. G. Dawber and R. J. Elliot, *Proc. Roy. Soc. London* **273**, 222 (1963).

⁷A. A. Maradudin, *Lattice Dynamics* (Benjamin, New York, 1969), p. 1.

⁸For an extensive catalog of FIR lines, see, for example, C. T. Gross, J. Kiess, A. Mayer, and F. Keilmann, *IEEE J. Quantum Electron.* **2**, 377 (1987).

⁹R. Orbach, *Phys. Rev. Lett.* **16**, 15 (1966).

¹⁰R. S. Meltzer, J. E. Rives, and G. S. Dixon, *Phys. Rev. B* **28**, 4786 (1983).

¹¹L. Godfrey, J. E. Rives, and R. S. Meltzer, *J. Lumin.* **18/19**, 929 (1979).

¹²R. Orbach and L. A. Vredevoe, *Physics* (Long Island City, NY) **1**, 91 (1964).

¹³R. Baumgartner, M. Engelhardt, and K. F. Renk, *Phys. Rev. Lett.* **47**, 1403 (1981).

¹⁴ $\Sigma(\Delta) = \rho(\Delta)\delta_{\text{FIR}}$, where $\rho(51.9) \approx 10^{20}\text{ (modes/cm}^3\text{)/cm}^{-1}$ is the density of states calculated from Ref. 10 and $\delta_{\text{FIR}} = 1.7 \times 10^{-2}\text{ cm}^{-1}$ is the bandwidth of our FIR laser.

¹⁵A. Hadni and P. Strimer, *Phys. Rev. B* **5**, 4609 (1972).